Dipole Antenna backed by 8-CBU AMC-EBG and 8-CBU FSS at 5.8 GHz

Siti Adlina Md Ali, Maisarah Abu and Hasnizom Hassan
Centre for Telecommunication Research and Innovation (CeTRI),
Faculty of Electronic and Computer Engineering (FKEKK),
Universiti Teknikal Malaysia Melaka (UTeM), Malaysia.
khalif5086@yahoo.com

Abstract— **This paper investigates the performances of dipole antenna, incorporated with and without 8-Connected Branches Uniplanar Artificial Magnetic Conductor-Electromagnetic Band Gap (8-CBU AMC-EBG) and 8 Connected Branches Uniplanar Frequency Selective Surface (8-CBU FSS) at 5.8 GHz. The designs are simulated on Arlon AD-350 with permittivity, ε_r = 3.50, thickness, h = 1.016 mm and tangent loss, δ = 0.0026. Due to the flexibility of the material used as a substrate, the effect of different angle is investigated. Both the 8-CBU AMC-EBG and 8 the CBU FSS act as a reasonably good ground plane for the dipole antenna and help to improve the realized gain and the radiation patterns by pushing the front lobe, while at the same time reducing the side lobes. The maximum improvements led by dipole antenna with 8-CBU AMC-EBG are 8.54 dB of realized gain is achieved and approximately 6.53 dBi of the directivity of front lobe is pushed higher than the dipole alone while the side lobe is significantly lower than with 8-CBU FSS. The designs of 8-CBU AMC-EBG and 8-CBU FSS can be applied to dipole antenna application such as Wi-fi and other on-body communication devices.**

Index Terms— **Artificial Magnetic Conductor (AMC), Electromagnetic Band Gap (EBG), Frequency Selective Surface (FSS), dipole antenna, and 8 Connected Branches Uniplanar AMC-EBG and 8 Connected Branches Uniplanar FSS**

I. INTRODUCTION

Recently, there has been a growing research interest to develop flexible system technology. Flexible antennas are the main method implemented in body centric communications [1],[2]. Recognizing that the use of flexible antennas on human causes performance distortions due to distinct properties of human body itself [3], research in flexible antennas has received a remarkable interest [4],[5].

Research activities in the field of antennas focus on the design of light-weight, conformable and small antennas [6-8] that could retain good radiation efficiency, while at the same time support large enough bandwidth to accompany the requirements of high data rates in modern communication systems. Extensive researches have been conducted in the printed antennas on flexible substrate and these researches have demonstrated that the presence of human body not only significantly affects the antenna radiation properties, but also gives rise to surface wave communication.

Printed antennas are frequently used due to their advantages such as light weight, ease of fabrication and compact size [8]. The antennas have relatively narrow bandwidth characteristics. An ultra-wideband (UWB) antenna has also been developed and it consists of printed planar dipole antenna. This type of antenna is suitable since it provides a large bandwidth and also give better polarization in comparison with other structures in addition to their low cost [9]. There many kinds of UWB antenna types such as bow-tie [10], TEM horn [11] and spiral [12].

For this research, printed dipole antenna is the best candidate for the flexible system since it is simple, easy to fabricate and easy [13] to integrate with AMC, FSS and EBG. It also comes in many different shapes. However, it is categorized as a low gain antenna, as it is fundamentally limited by the size, radiation patterns and the frequency operation.

When placed on human body, flexible antennas itself experience performance degradation, such as frequency detuning, bandwidth reduction and radiation distortions. Moreover, the radiation that penetrates into the human cells is a major health concern [3]. One way to improve the overall antenna performance is to enhance the gain of a system at receiver end, and this can be achieved by using AMC, FSS and EBG. All the three meta-materials above have been used extensively in the past for enhancing the performance of antennas by improving the gain and reducing the radiation exposure to the human body [15-18].

In [19], the realized gain is improved up to 2.1 dBi. Additionally, paper [20] concluded that placing the EBG behind the antenna considerably reduces back radiation by at least 13 dB while improving gain by up to 3 dB in a direction away from the body. Furthermore, analysis in [21] found that the maximum gain enhancement is around 7.5 dB and the average gain enhancement is more than 4 to 5 dB for the complete operational band.

In this paper, the performances of dipole antenna backed with 8-CBU AMC-EBG and 8-CBU FSS are evaluated at 5.8 GHz. The performances improvement of dipole antenna while incorporating with 8-CBU AMC-EBG and 8-CBU FSS are investigated on the flexible materials and their performance in terms of angle of incidence. All the design simulations are done using Computer Simulation Technology (CST) Microwave Studio software. Both AMC and FSS act as a reasonably good ground plane for the dipole antenna and help to improve the realized gain and push the front lobe of the radiation patterns of the dipole antenna.

II. 8-CBU AMC-EBG DESIGN

This section describes the designs of 8-CBU AMC-EBG that are incorporated with the dipole antenna. As the initial design, the properties of the square patch AMC are investigated followed by the 8-CBU AMC-EBG operating at 5.8 GHz.

A. Square patch AMC design at 5.8 GHZ

This section describes the design of 5.8 GHz square patch AMC that is capacitive square patch frequency selective surface (FSS) backed by a ground plane with 0.035 mm thickness. This AMC is designed using the substrate parameters; permittivity ε_r = 3.5, thickness h = 1.016 mm and tangent loss δ = 0.0026. The characteristics of the AMC such as the reflection phase, reflection magnitude and surface impedance of the AMC are simulated using frequency solver in CST Microwave Studio.

As in [22], the inductance (L), capacitance (C), frequency response (f_r) and bandwidth (BW) of the equivalent circuit for mushroom EBG structure are based on the following equations:

$$L = \mu_o h, \tag{1}$$

$$C = \frac{W\varepsilon_O(1 + \varepsilon_R)}{\pi} cosh^{-1}\left(\frac{2W + g}{g}\right) \tag{2}$$

$$f_r = \frac{1}{2\pi\sqrt{LC}} \tag{3}$$

$$BW = \frac{1}{\eta_O}\sqrt{\frac{L}{C}} \tag{4}$$

where η_o, ε_o and μ_o are the impedance, permittivity and permeability of free space, w is the patch width and g is the gap between adjacent patches. At resonance, the surface impedance Z_s is determined by:

$$Z_S = \frac{jwL}{1 - w^2LC} \tag{5}$$

Basically, the square shape of AMC is about 56.40 mm with 1 mm gap between the patches. The unit cell and the reflection phase of 5.8 GHz square patch AMC are shown in Figure 1. The designed AMC has a patch width of mm and the gap between the elements is mm. Based on Equation 1 to 3, the calculated AMC resonant frequency is GHz, where C is 0.61 pF and L is 0.63 nH. Then, the surface impedance at resonance is determined using Equation 5 with the occurrence of both capacitance and inductance.

As shown in Figure 1, the reflection phase varies from 180° to -180°. At resonance, which is at 5.8 GHz, the reflection phase is 0° while at ±90° of reflection phase, the frequency is laid between 5.77 GHz to 5.83 GHz, thus contributes to 1.03% bandwidth. Furthermore, the square patch AMC has a reflection magnitude of -4.54 dB, which corresponds to 0.59.
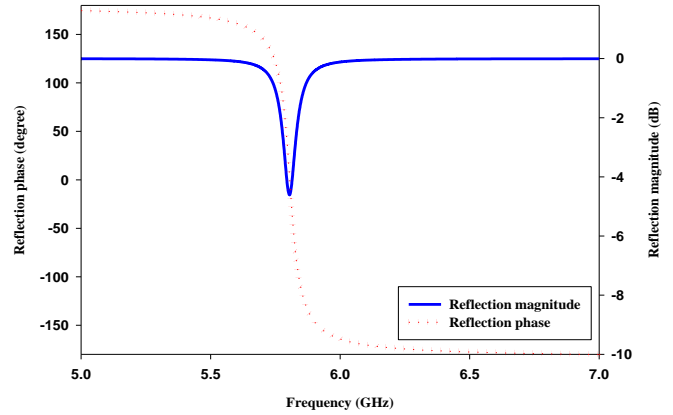

Figure 1: The reflection phase and magnitude of unit cell square patch AMC design at 5.8 GHz:

B. 8-CBU AMC-EBG design at 5.8 GHZ

One of the most important considerations in designing the 8-CBU AMC-EBG is to make sure that the structure evaluates both the AMC and EBG characteristics. The reflection phase of the design should vary from 180° to -180° and the resonance frequency is at the 0° reflection phase. Furthermore, the structure also should have a band gap at the resonance frequency.

Basically the 8-CBU AMC-EBG structure involves a square shape of substrate with a main square patch at the center of the substrate, while the main square patch is connected with eight branches and each of the four of them has a corner square connected at the end of the branch. All the branches are designed alternately between the basic branches with the connected corner square branches. Furthermore, each branch is designed at the center of each length of the main square.

Notice that the capacitance is introduced by the gaps between the neighboring patches and the inductance is provided by the narrow branches. The series inductors combined with the shunt capacitors constitute an array of parallel *LC* circuits, thus it has a high surface impedance at the resonant frequency. The 8-CBU AMC-EBG structure is shown in Figure 2, and Table 1 defines the technical description and dimensions of the structure.
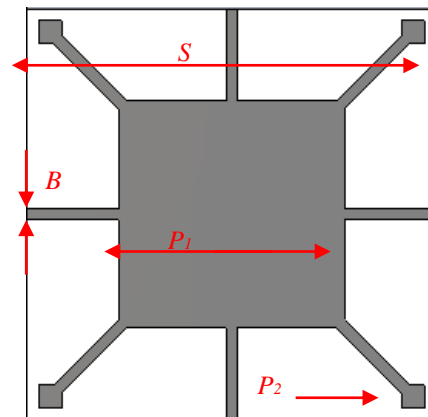

Figure 2: 8-CBU AMC-EBG design at 5.8 GHz

Table 1
Technical descriptions and dimension a unit cell of 8-CBU AMC-EBG at 5.8 GHz

Description	Design Parameter	Dimension (mm)
Branch width	*B*	0.46
Main-square length	*P*	9.20
Sub-square length	*Z*	0.92
Square substrate length	*M*	16.56

The simulated reflection phase and magnitude and the surface impedance are plotted in Figure 3(a) and (b) respectively. The reflection phase varies from 180° to -180°. At 5.8 GHz, the reflection phase is 0° and at ±90° reflection phase, the frequency is laid between 5.77 GHz to 5.82 GHz. The reflection magnitude is -1.27 dB corresponding to 0.86 and has a very high impedance at the resonant frequency.

The bandwidth of the structure is evaluated from the reflection phase diagram of the 8-CBU AMC-EBG and square patch AMC at 5.8 GHz. Based on±90°, the computed bandwidth of the 8-CBU AMC-EBG is 3.34%, while the bandwidth of square patch AMC is 2.31%, lower than 8-CBU AMC-EBG. However, the 8-CBU AMC-EBG configuration produces a reduction of almost half of size than the square patch AMC.
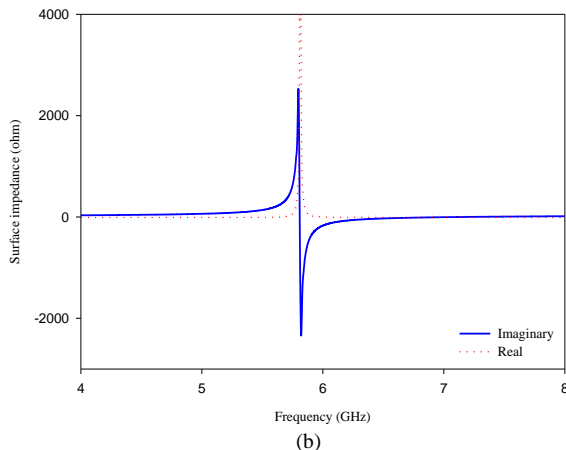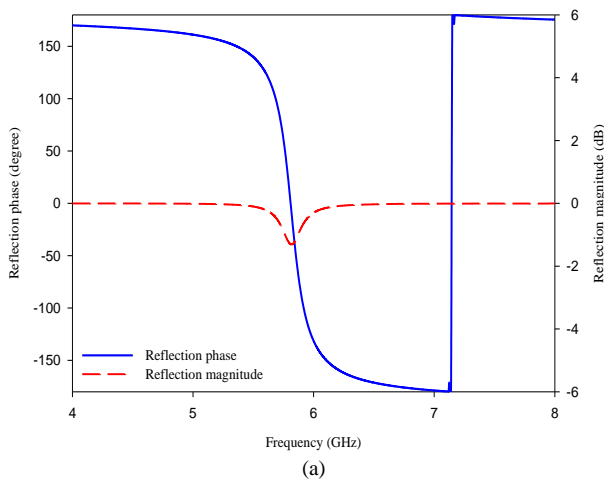

(a)

(b)

Figure 3: Unit cell of 8-CBU AMC-EBG design at 5.8 GHz: (a) reflection phase and magnitude, and (b) surface impedance.

Due to the flexibility and the very thin substrate's material, the effect of different angle is investigated [23]. Thus, the different bending angle of the structure is significantly affected by the performances of the 8-CBU AMC-EBG. Otherwise, the structure has high angular stability due to the resonance frequency that did not really affected by the changes of incident angle. Figure 4 shows the reflection phase of the 8-CBU AMC-EBG with different incidence angle. From the observation, the frequency response of the structure was not affected by the changes of incidence angle; thus, the 8-CBU AMC-EBG has high angular stability.
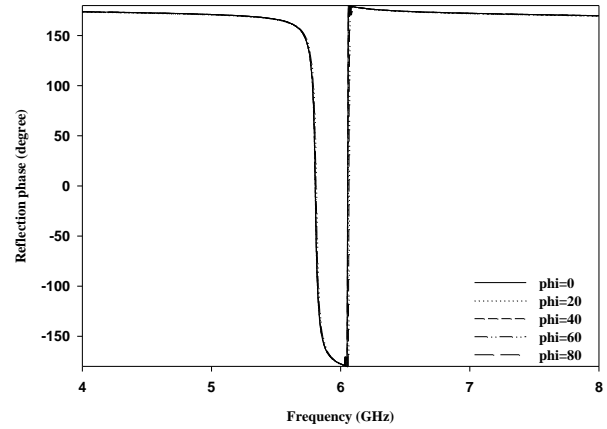

Figure 4: Reflection phase of the 8-CBU AMC-EBG at 5.8 GHz with different incidence angle

Besides, this paper also investigates the occurrence of the band gap from the 8-CBU AMC-EBG design. In order to characterize the band gap, 10 x 6 arrays of 8-CBU AMC-EBG is built. The method of suspended 50 Ω micro-strip line [24-25] is applied through time domain solver of CST. The supporting material and suspended line layers are added to the basic layers of 8-CBU AMC-EBG that consist of patch, substrate and ground. Two 50 Ω SMA connectors are located at both ends of the transmission line to transmit and receive Electromagnetic (EM) waves.

Figure 5 illustrates the transmission and reflection of the 10x6 arrays of 8-CBU AMC-EBG. The results show that the structure has successfully achieved a band gap at 5.8 GHz. Based on -20 dB transmission value, the band covers from 4.64 GHz to 7.46 GHz. As long as the resonance frequency falls into this band gap frequency range, the surface wave can be suppressed while the antenna is incorporated with this structure.

III.   8-CBU FSS DESIGN

A.   8-CBU AMC-EBG without ground plane

FSS structure involves the patch and substrate layers only as compared to AMC which involves the patch, substrate and ground layers. 8-CBU AMC-EBG without the ground plane evaluates transmission and reflection curves at a higher operating frequency as shown in Figure 6. Therefore, the structure needs to be bigger in order to evaluate the transmission at the desired resonate frequency, 5.8 GHz.
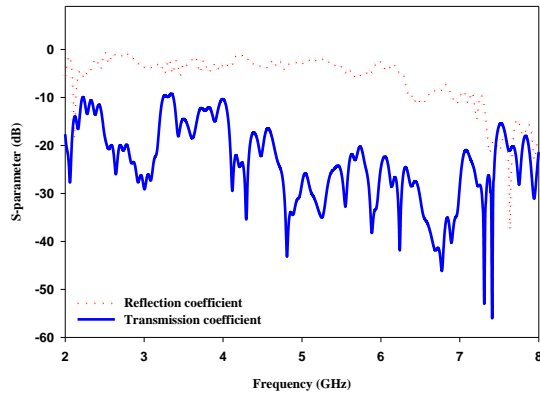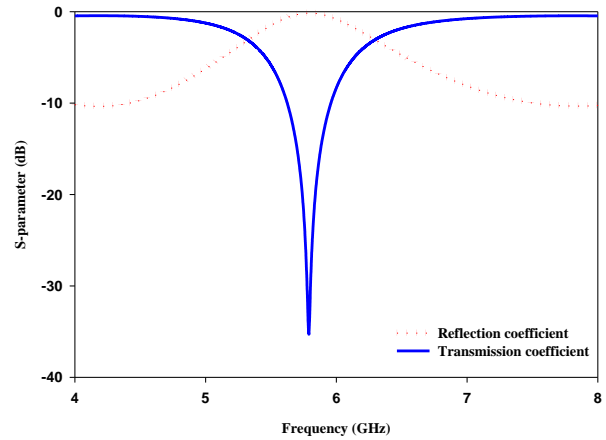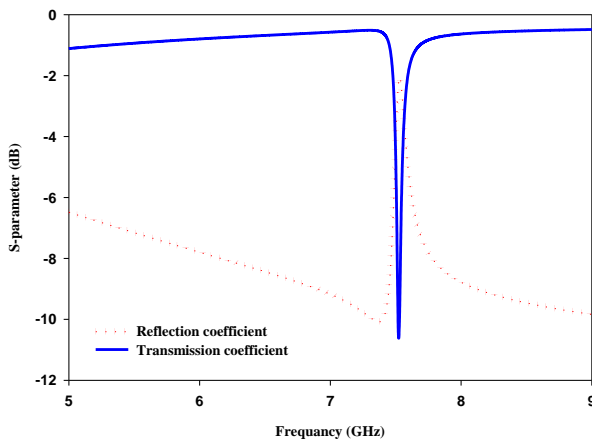
Figure 5: Band Gap of 8-CBU AMC-EBG

Figure 6: Transmission and reflection curves of 8-CBU AMC-EBG

B. *8-CBU FSS design at 5.8 GHZ*

Basically, the design structure of 8-CBU FSS and 8-CBU AMC-EBG is exactly the same but with different overall size. The structure of 8 CBU FSS is bigger than 8-CBU AMC-EBG and Table 2 shows the technical descriptions and dimensions of the unit cell of 8-CBU FSS at 5.8 GHz.

Table 2
Technical descriptions and dimension a unit cell of 8-CBU FSS at 5.8 GHz.

Description	Design Parameter	Dimension (mm)
Branch width	B	2
Main-square length	P	41.08
Sub-square length	Z	4
Square substrate length	M	52

The simulated transmission and reflection curves are plotted in Figure 7. From the plotted graph, the 8-CBU FSS evaluates -31.28 dB of the transmission and reflection for about -0.11 dB at 5.8 GHZ. Based on -10 dB, the frequency is laid from 5.62 GHz to 5.96 GHz; thus, computed bandwidth of the 8-CBU FSS is 5.86%.
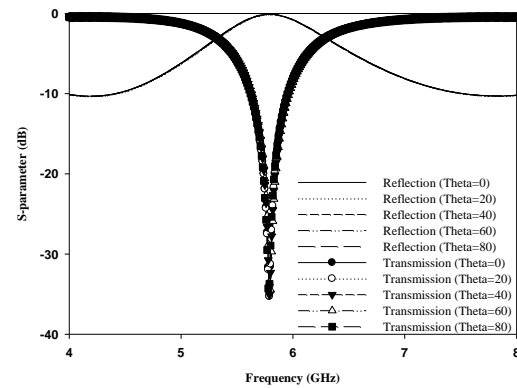

Figure 7: Transmission and reflection curves of unit cell 8-CBU FSS at 5.8 GHz

Similar to 8-CBU AMC-EBG, the effect of the different angle is investigated. The reflection phase of the 8-CBU FSS with different incidence angle is plotted in Figure 8. From the observation, the frequency response of the structure was not affected by the changes of incidence angle; thus, the 8-CBU FSS has high angular stability.

Figure 8: Transmission and reflection curves of the 8-CBU FSS at 5.8 GHz with different incidence angle.

IV. PRINTED DIPOLE ANTENNA DESIGN AT 5.8 GHz

In this section, the basic design of dipole antenna is designed at 5.8 GHz. The radiating elements which are made of Perfect Electromagnetic Conductor (PEC) with 0.035 mm thickness are printed on a flexible material. The flexible material used is Fast Film with a thickness of 0.13 mm, dielectric constant of 2.7 and tangent loss of 0.0012. Both radiating elements are connected to the 50 Ω Sub Miniature Version A (SMA) connector as shown in Figure 8 (a). While Figure 9 (b) shows the simulated and measured return loss of the dipole antenna at 5.8 GHz. Both simulated and measured results agree to each other.
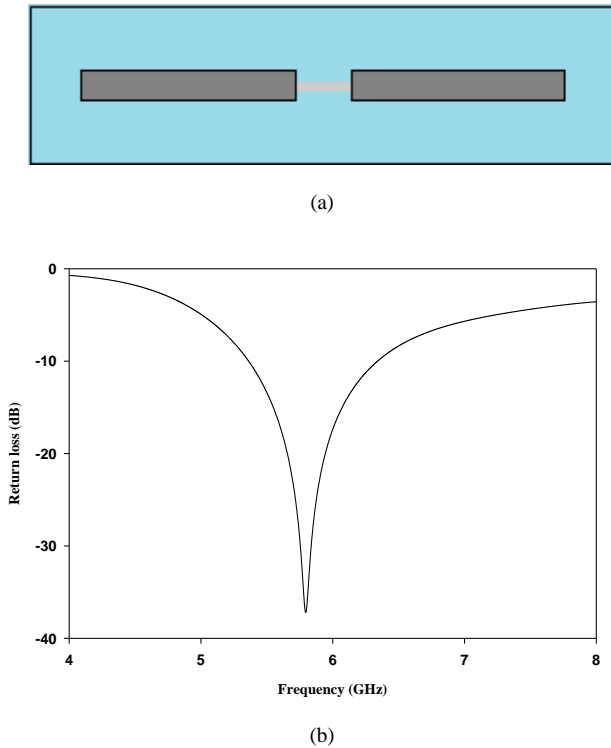
(a)

(b)

Figure 9: Dipole antenna at 5.8 GHz: (a) the fabricated dipole antenna, and (b) the simulated and measured return loss of the dipole antenna.

V. DIPOLE ANTENNA WITH 8 CBU AMC-EBG AND 8 CBU FSS

The performances of the dipole antenna with 8-CBU AMC-EBG and 8-CBU FSS are investigated in this section. The configurations of the dipole antenna with 8-CBU AMC-EBG and 8-CBU FSS are given in Figure 10. The 8-CBU AMC-EBG and 8-CBU FSS are placed below the antenna with a certain gap distance. Both of them act as a reasonably good ground plane for the antenna when impedance is very low. Thus, all the capacitive components more or less cancel all of the inductive components and achieved a very low transmission coefficient and in phase reflection over entire bandwidth. The gap is maintained by using a special material, Rohacell 31HF with dielectric constant of 1.05. This material is used as a spacer between the antenna and the AMC and FSS surface.

A. Dipole antenna with 8-CBU AMC-EBG

The 10x6 arrays of 8-CBU AMC-EBG is developed in order to incorporate with the dipole antenna. The gap between the antenna and 8-CBU AMC-EBG surface is maintained at 3 mm. Figure 11 illustrates the return loss of dipole antenna with and without 8-CBU AMC-EBG, there is a shifting in resonance although the antenna still performs well at 5.8 GHz. The dipole alone produces around -38 dB of return loss, while the present of 8-CBU AMC-EBG has around -31 dB of return loss at 5.8 GHz.
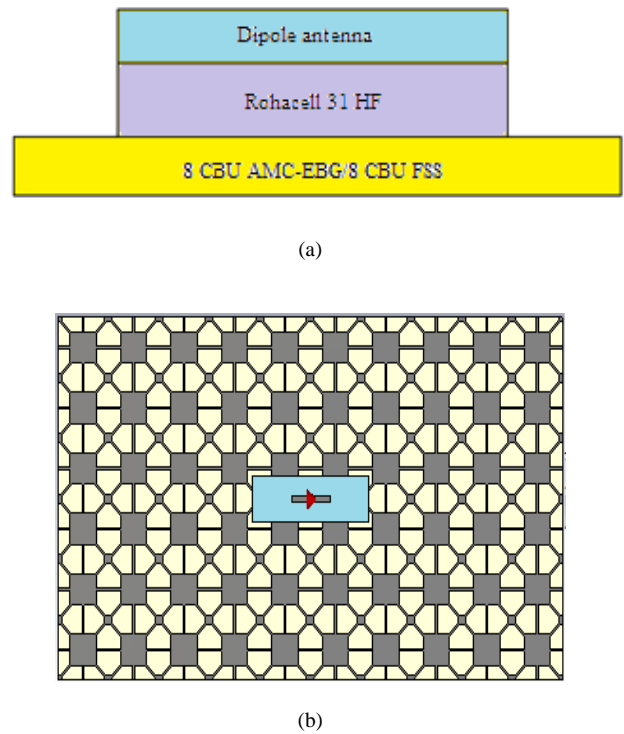

(a)

(b)

Figure 10: The configurations of the dipole antenna with 8-CBU AMC-EBG and 8-CBU FSS: (a) side view, and (b) front view
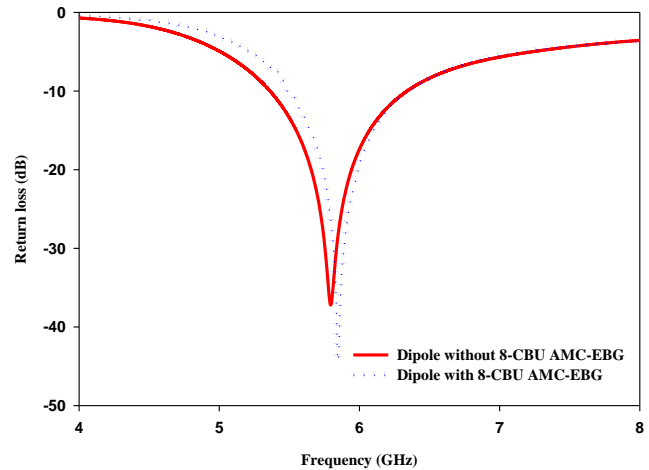

Figure 11: The simulated and measure return loss of dipole antenna with and without 8-CBU AMC-EBG.

The Cartesian plot of the dipole antenna with and without 10x6 arrays of 8-CBU AMC-EBG is plotted in Figure 12. An interesting finding is the significant increase of directivity. The front lobe is improved by 6.50 dBi, while the back lobes is reduced around 20 dBi. The absence of 8-CBU AMC-EBG which has in phase image currents with the antenna current contributes to the directivity improvements. Then, 8-CBU AMC-EBG acts as a reflector and reflects the back lobes of the radiation to be directive and increases the front lobes at the same time. The radiation pattern of the antenna is improved by increasing the front radiation and reducing the side radiation.
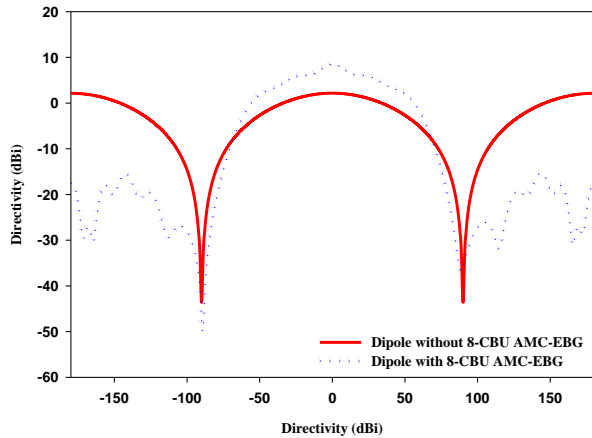
Figure 12: The Cartesian plot of the dipole antenna with and without 8-CBU AMC-EBG

B. *Dipole Antenna with 8-CBU FSS*

The 5x3 arrays of 8-CBU FSS is built to incorporate with the dipole antenna. The gap is also maintained at 3 mm. The plotted return loss of dipole antenna with and without 8-CBU FSS is shown in Figure 13. Similar to 8-CBU AMC-EBG, there is a shift in resonance. Despite of the shifting, the dipole antenna still performs well at 5.8 GHz. −38 dB of return loss achieved by dipole alone, while the incorporation with 8-CBU FSS produces around -21 dB of return loss.
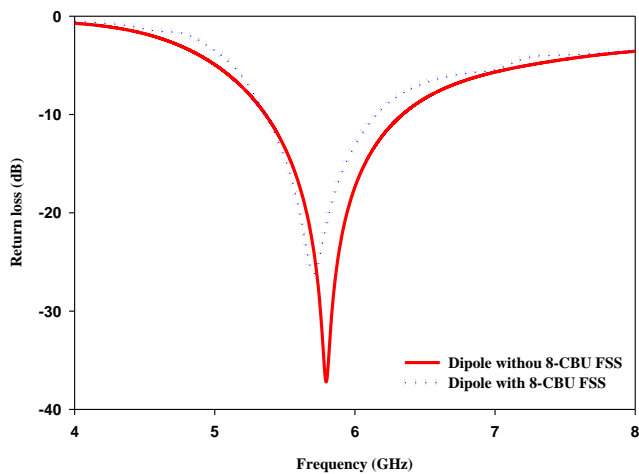

Figure 13: The simulated and measure return loss of dipole antenna with and without 8-CBU FSS

Figure 14 (a) shows the Cartesian plot of the dipole antenna with and without 8-CBU AMC-EBG and 8-CBU FSS. The front radiation of the antenna is directed and the side radiation is reduced at the same time, when it is incorporated with both structures. However, with 8-CBU AMC-EBG, the front lobe is pushed higher and the side lobe is significantly lowered when it is with 8-CBU FSS. Figure 14 (b) illustrates the polar plot of the dipole antenna with and without 8-CBU AMC-EBG and 8-CBU FSS. Note that both 8-CBU AMC-EBG and 8-CBU FSS reduce the back lobes of the radiation pattern; thus, it is very important when applying this structure on the body. Moreover,

the radiation that penetrates into the human cells is one of the major health concerns.
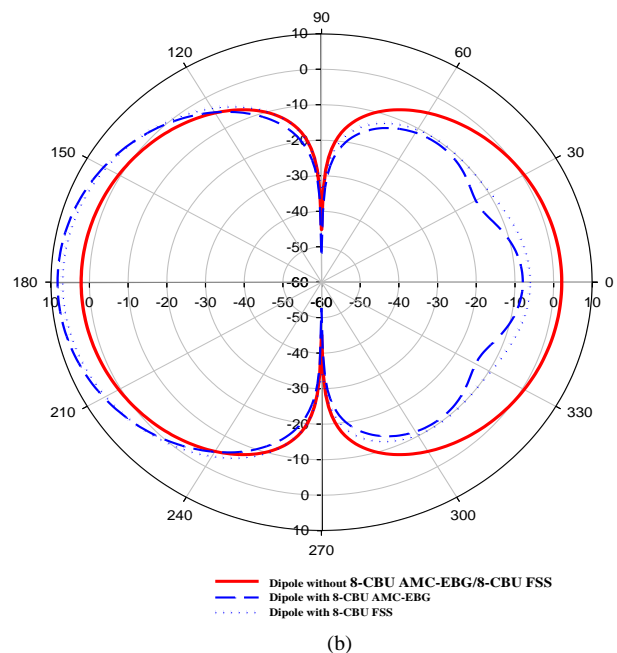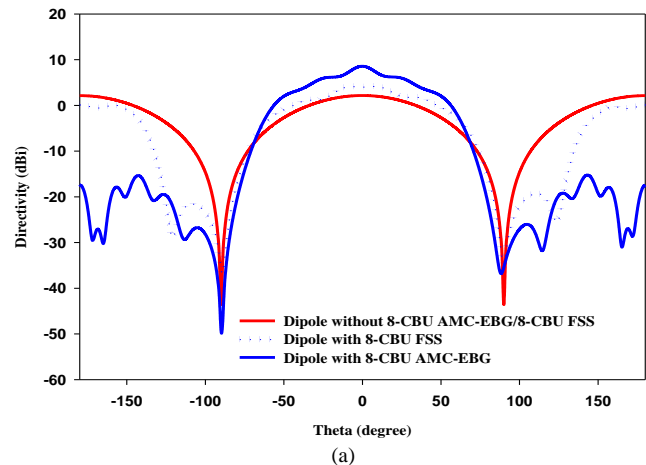

(a)

(b)

Figure 14: The dipole antenna with and without 8-CBU AMC-EBG and 8-CBU FSS; (a) Cartesian plot b) Polar plot

C. *Performances summary of dipole with 8-CBU AMC-EBG and 8-CBU FSS*

The vertical bar chart in Figure 15 shows the performances summary of the dipole antenna with and without 8-CBU AMC-EBG and 8-CBU FSS. The plotted bar chart shows that the interesting finding is the significant increase of realized gain and directivity. From the observation, dipole antenna alone has an omni-directional radiation pattern; thus, the directivity and realized gain for the front and back lobes will be the same, as shown in Figure 14 (b). Thus, there are approximately 2.01 dB of realized gain and approximately 2.015 dBi of directivity. The presence of both 8-CBU AMC-EBG and 8-CBU FSS improves both the directivity and realized gain of the antenna. Dipole with 8-CBU AMC-EBG leads high increment for both realized gain and directivity around 8.54 dB and 8.54 dBi respectively.

As in Figure 14, the front lobe is pushed higher and the side lobe is significantly lowered than with the 8-CBU FSS. Thus, the aim of this research is achieved, which is to improve the realized gain and improve the radiation patterns by pushing the front lobe while at the same time reducing the side lobes.
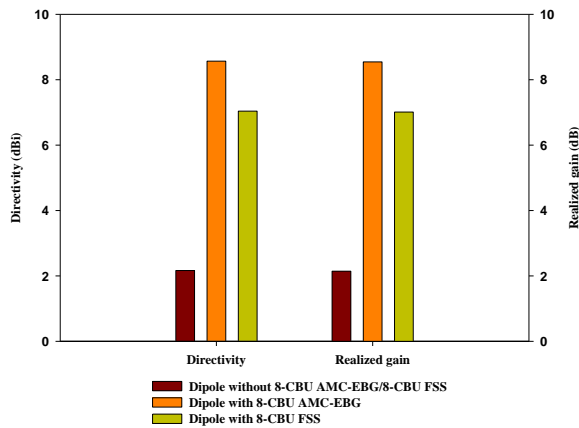

Figure 15: The comparison of performances dipole antenna with and without 8-CBU AMC-EBG and 8-CBU FSS

VI. CONCLUSION

The performances improvement of dipole antenna while incorporating with 8-CBU AMC-EBG and 8-CBU FSS are successfully designed on the flexible materials and their performance in terms of angle of incidence are studied. Both 8-CBU AMC-EBG and 8-CBU FSS act as a reasonably good ground plane for the dipole antenna and help to improve the realized gain and the radiation patterns by pushing the front lobe, while at the same time reducing the side lobes. The maximum improvements led by the dipole antenna with 8-CBU AMC-EBG are 8.54 dB of realized gain achieved and around 6.53 dBi of directivity of the front lobe is pushed higher than the dipole alone while the side lobe is significantly lowered than with 8-CBU FSS. Such a directive antenna is very important to be applied on-body applications and is a major health concern as the radiation that penetrates into human cells. The designs of 8-CBU AMC-EBG and 8-CBU FSS can be applied to dipole antenna application, such as Wi-fi and others on-body communication devices.

ACKNOWLEDGMENT

REFERENCES

[1] G. Adamiuk, T. Zwick, and W. Wiesbeck, "UWB Antennas for Communication Systems," *Proceeding of the IEEE*, 100(7), 2012.
[2] D. Cara, D. Trajkovikj, J. Torres-sánchez, R. Zürcher, and J. Skrivervik, "A Low Profile UWB Antenna for Wearable Applications : The Tripod Kettle Antenna (TKA)," *European Conference on Antennas and Propagation (EuCAP)*, 2013, pp. 3257–3260.
[3] J. Choi, J. Tak, and K. Kwon, "Low-Profile Antennas for On-Body Surface Communications," *International Workshop on Antenna Technology*, 2014, pp. 288–29.
[4] D. Cure, T. Weller, and F. A. Miranda, "Study of a Flexible Low Profile Tunable Dipole Antenna Using Barium Strontium Titanate Varactors," *The 8th European Conference on Antennas and Propagation (EuCAP 2014)*, 2014, pp. 31–35.
[5] P. Duangtang, P. Krachodnok, and R. Wongsan, "Gain Improvement for Conventional Conical Horn By Using Mushroom-like Electromagnetic Band Gap," *Electrical Engineering/Electronics, Computer, Telecommunications and Information Technology (ECTI-CON)*, 2014, pp. 3–6.
[6] O. M. Haraz, Abdel-rahman, M. Alshebili, and S. A. Sebak, "A Novel 94-GHz Dipole Bow-tie Slot Antenna on Silicon for Imaging Applications," *IEEE Asia-Pacific Conference on Applied Electromagnetics (APACE)*, 2014, pp. 8–10.
[7] Ilarslan, M. Aydemir, M. E. Gose, and E. Turk, "The Design and Simulation of a Compact Vivaldi Shaped Partially Dielectric Loaded (VS-PDL) TEM Horn Antenna for UWB Applications," *IEEE International Confrence on Ultra - Wideband (ICUWB)*, pp. 23–26, 2013.
[8] B. Ivsic, G. Golemac, and D. Bonefacic, "Performance of Wearable Antenna Exposed to Adverse Environmental Conditions," *Apllied Electromagnetics and Communications (ICECom)*, 2013, pp. 978-953.
[9] Z. H. Jiang, D. E. Brocker, P. E. Sieber, and D. H. Werner, "A Compact , Low-Profile Metasurface-Enabled Antenna for Wearable Medical Body-Area Network Devices," *IEEE Transaction on Antennas and Propagation*, 2014, pp. 4021–4030.
[10] K. Kamardin, M. K. A. Rahim, and P. S. Hall, "Textile Diamond Dipole and Artificial Magnetic Conductor Performance under Bending , Wetness and Specific Absorption Rate Measurements," *Radio Engineering*, 2015, pp. 729–738.
[11] S. Koziel, S. Ogurtsov, W. Zieniutycz, and A. Bekasiewicz, "Fast Simulation-Driven Design of a Planar UWB Dipole Antenna with an Integrated Balun," *Antenna and Propagation (EuCAP 2015)*, 2015.
[12] S. Y. Lin, Y. C.Lin, and Y. T. Pan, "UWB Planar Dipole Antenna with Notched Band," *International Symposium on Antennas and Propagation (ISAP)*, 2014, pp. 333–334.
[13] N. Liu, P. Yang, and W. Wang, "Design of a Miniaturized Ultra-wideband Compound Spiral Antenna," *Microwave Technology & Computational Electromagnetics (ICMTCE)*, 2013, pp. 1–4.
[14] E. Moradi, K. Koski, M. Hasani, and L. Ukkonen, "Antenna Design Considerations for Far Field and Near Field Wireless Body-Centric Systems," *Computational Electromagnetics (ICCEM)*, 2015, pp. 59–60.
[15] M. Nafe, A. Syed, and A. Shamim, "Gain Enhancement of Low Profile On-chip Dipole Antenna Via Artificial Magnetic Conductor At 94 GHz," *Antennas and Propagation (EuCAP)*, 2015.
[16] S. Pimpol, "Band-Notched Printed Dipole Antenna with EBG Reflector," *IEEE*, 2014.
[17] S. Shadrokh, Y. Y. Qiang, F.Jolani, and Z. Z. Chen, "Ultra-compact End-loaded Planar Dipole Antenna for Ultra-wideband Radar and Communication Applications," *Electronic Letters*, 2014, pp. 1495–1496.
[18] M. Abu, and M. K. A. Rahim, "Single-band and Dual-band Artififcial Magnetic Conductor Ground Planes for Multi-band Dipole Antenna," *Radio Engineering*, 2012, Vol. 21, No. 4.
[19] R. Dewan, S. K. A. Rahim, S. F. Ausordin, D. N. A. Zaidel, B. M. Sa'ad, and T. Purnamirza, "Bandwidth Widening, Gain Improvement and Efficiency Boost of an Antenna using AMC Ground Plane," *Jurnal Teknologi*, 2014, pp. 2180-3722.
[20] S. Zhu, and R. Langley, "Dual-Band Wearable Antennas over EBG Substrate," *Electronic* Letters, 2007, Vol. 43, No. 3.
[21] H. N. Aqeel, and A. T. Farooq, "A Super Wideband Printed Antenna with Enhanced Gain using FSS structure," *Proceedings of 12th International Bhurban Conference on Applied Science & Technologhy (IBCAST)*, 2015, 978-1-4799-6369-0/15.
[22] Razali, R. "Comparison between Electromagnetic Band Gap, Artificial Magnetic Conductor and Frequency Selective Surface," *Degree Thesis of Universiti Teknikal Malaysia Melaka*, 2014.

[23] M. Abu, E. E. Hussin, R. F. Munawar and H. Rahmalan, "Design Synthesis of 5.8 GHz Octagonal AMC on a Very Thin Substrate," *Internatinal Journal of Information and Electronics Engineering*, 2015.

[24] M. Abu, and M. K. A. Rahim, "Single-band Zigzag Dipole Artificial Magnetic Conductor," *Jurnal Teknologi*, 2012.

[25] O. Ayop, M. K. A. Rahim, M. Abu, and T. Masri, "Slotted Patch Dual Band Electromagnetic Band Gap Structure Design," *3rd European Conference on Antenna and Propagation (EUCAP)*, 2009, pp. 2618-2621.